

## THE APPLICATION OF MODIFIED PHASE EXTRACTED BASIS FUNCTIONS IN SCATTERING ANALYSIS OF DIELECTRIC-COATED TARGETS

X. Niu\*, Z. Nie, and S. He

Department of Microwave Engineering, School of Electronic Engineering, University of Electronic Science and Technology of China (UESTC), Chengdu 611731, China

**Abstract**—A novel basis function, called as the Modified Phase Extracted (MPE) basis function, has been proposed to analyze three-dimensional scattering problems for electrically large, thin dielectric-coated targets. The MPE basis function, which can be defined on large (e.g., a wavelength or more) curvilinear geometrical elements, is developed for quadrilateral cells. Consequently, combining with the thin dielectric sheet (TDS) approximation, the MPE basis function solves the scattering problem accurately with fewer unknowns than the solutions based on the conventional basis functions. In order to improve the accuracy of the solution solving the problem which has thicker dielectric coatings, some modifications about the TDS approximation model are made. Numerical examples demonstrate that the validity of the proposed approach in solving the scattering from electrically large, thin coated objects.

### 1. INTRODUCTION

The efficient simulation of electromagnetic scattering from electrically large, coated targets has practical value for the engineering application, such as the analysis of scattering from antennas with dielectric radomes, radar stealth and anti-stealth. Because of the coupling relationship between the conductor and the dielectric, there are numerous computational complexities and memory requirement in the calculation. Various numerical methods, such as the Volume Integral Equations (VIEs) [1], the Surface Integral Equations (SIEs) [2, 3], and the Impedance Boundary Condition (IBC) [4], have been developed to treat this kind of problem.

---

*Received 28 February 2012, Accepted 23 March 2012, Scheduled 11 April 2012*

\* Corresponding author: Xue Niu (niuxue5@gmail.com).

Considering the electromagnetic boundary conditions and the equivalence principle, the integral equation method is a strict numerical solution. Located in the volume, the equivalent currents are considered as the unknowns in the VIEs. Such a method is not applicable for an electrically large scatterer due to a great many unknowns. Different from the VIEs, the unknown currents are distributed on the surface of the object in the SIEs, but there is poor convergence efficiency analyzing the dielectric-coated targets [5]. Another commonly used method, the IBC is known as an efficient technology in solving electromagnetic scattering problems involving coated bodies. Unfortunately, the specific criteria limit the range of the IBC validity. The impedance must be approximated assuming that the object is locally flat, or measured by experiments. These constraints lead to complicated integral operators and some errors which cannot be ignored.

In this case, the TDS [6–8] approximation is presented. As a powerful progress in the computational electromagnetics (CEM), the TDS approximation is a reliable method in the analysis of thin dielectric-coated scatters. When the thickness of the dielectric is thin enough compared with the dielectric wavelength or the skin depth, the scattering problem can be dealt with the TDS efficiently. Moreover, it is easy to accomplish numerical simulations about the locally coated object. The TDS approximation simplifies the scattering model to a great extent. Based on the approximate model, unfortunately, the TDS is not suitable for the object with thicker dielectric coatings. Furthermore, it is still time-consuming due to a great number of unknowns, especially for the electrically large objects.

To improve the computational efficiency, the development of new basis functions with few unknowns is an alternative method. The traditional lower order basis functions defined on the triangular or quadrilateral elements, such as the Rao-Wilton-Glisson (RWG), Roof-top basis functions, need about 150 unknowns per wavelength squared for metallic surfaces. For the higher order hierarchical basis functions, there are only about 30 unknowns per wavelength squared for the same object [9]. Nevertheless, even for the well-designed current expansions, the number of unknowns for electrically large structures can be so large that the memory consumption will be too huge.

By containing propagating wave phase dependence, the phase extracted (PE) basis function [10] can be defined on curvilinear triangular patches with electrical size much larger than the other traditional bases for closed metallic scatters. As we know, there are not only traveling waves but also standing wave components in the currents over the surface. Unlike the scatterer which has a simple

shape, the induced current changes rapidly on the surface of the complex object. When the current varies rapidly, the standing wave component cannot be ignored. Following this direction, the MPE basis function is presented. The new basis function is applicable to scattering problems not only the convex objects but also the concave objects which have strong mutual couplings. By using MPE basis functions, even without the Multilevel Fast Multipole Methods (MLFMA) [11], integral equations would be solved with the MoM efficiently. And the number of unknowns, memory usage, and computational time can be reduced significantly compared with traditional basis functions. However, the MPE basis function is only used to solve scattering from the perfect electric conductor (PEC) before. This is the first time to introduce the MPE basis function in the analysis of the dielectric-coated targets.

The emphasis of this paper is to analyze the electrically large, thin dielectric-coated scatters with the approach based on the combination of MPE basis functions and the TDS approximation. Also, a further research on the analysis of thicker dielectric coatings is studied. In order to solve the scattering from objects with thicker dielectric coatings, the modified TDS approximation is presented. The approximation error caused by the conversion from the VIE to the SIE, mainly reflects on the application of Green's functions. Thus, several modifications on the Green's function are made. Compared with the traditional TDS, the modified solution proposed in the paper improves the accuracy of the scattering problem for thicker dielectric-coated objects without increasing unknowns.

This paper is organized as follows. Firstly, the construction of the MPE basis function is reviewed and the associated current distribution over the surface is discussed in Section 2. Section 3 presents the application of the MPE basis function in scattering from thin dielectric-coated objects based on combining with the TDS approximation. It also involves a consideration of the expansion order adapted to the electrical size of the patch for a coated spherical scatterer. Three numerical comparisons with existing solutions are shown to demonstrate the good accuracy. In Section 4, some modifications about the TDS approximation are made. The scattering calculation for a thicker coated sphere shows the validity of the modification. Finally, the conclusion of the work is given in Section 5.

## 2. THE MPE BASIS FUNCTION

For the hierarchical basis function, the basis of order  $M$  is a subset of the basis of order  $M + 1$ , which causes different expansion orders on

different patches with the same mesh. Therefore, arbitrary hierarchical basis includes the lower order basis, e.g., RWG or Roof-top, as the lowest order member of the basis. Based on the characteristic, hierarchical bases have the advantages of both lower order and higher order bases in a single basis function.

Considering the hierarchical feature, the improvement of PE basis functions becomes possible. By using the PE basis function as the lowest order one of the higher order hierarchical basis function which is defined on quadrilateral patches, the MPE basis function has been obtained. The higher order hierarchical Legendre basis functions [12, 13] maintain their oscillating capability by showing the standing wave distribution in their definition domains. PE basis functions gain their capability through describing the traveling wave phase dependence of the induced current. As a result, the new basis function has both the ability to describe the traveling wave and standing wave components.

## 2.1. Formulation of the MPE Basis Function

Consider a curved quadrilateral patch with the associated parametric curvilinear coordinate system defined by  $-1 \leq u, v \leq 1$ . Consequently, the induced current on the surface is expanded as follows:

$$\mathbf{J}(\mathbf{r}) = \mathbf{J}(u, v) = J^u \mathbf{u} + J^v \mathbf{v} \quad (1)$$

where  $\mathbf{u} = \frac{\partial \mathbf{r}}{\partial u}$  and  $\mathbf{v} = \frac{\partial \mathbf{r}}{\partial v}$ . By interchanging  $u$  and  $v$ , the  $v$ -directed current can be derived because of the understanding above. The  $u$ -directed current is expanded as

$$\begin{aligned} J^u &= \frac{1}{\mathcal{J}(u, v)} \sum_{m=0}^1 \sum_{n=0}^{N^v} b_{mn}^u \tilde{C}_m \tilde{P}_m(u) C_n P_n(v) e^{i\mathbf{k}^i \cdot \mathbf{r}} \\ &+ \frac{1}{\mathcal{J}(u, v)} \sum_{m=2}^{M^u} \sum_{n=0}^{N^v} b_{mn}^u \tilde{C}_m \tilde{P}_m(u) C_n P_n(v) \end{aligned} \quad (2)$$

where  $b_{mn}^u$  is the unknown coefficient,  $\mathcal{J}(u, v) = |\mathbf{u} \times \mathbf{v}|$  is the surface Jacobian factor.  $\tilde{P}_m(u)$  and  $P_n(v)$  are the expansion polynomials.  $P_n(v)$  is the Legendre polynomial

$$P_n(v) = \frac{1}{2^n n!} \frac{d^n}{dv^n} (v^2 - 1)^n \quad (3)$$

that satisfies the orthogonality relation.

$$\int_{-1}^1 P_i(v) P_j(v) dv = \frac{2}{2i+1} \delta_{ij} \quad (4)$$

where  $\delta_{ij}$  is the Kronecker delta function. And the modified Legendre polynomial

$$\tilde{P}_m(u) = \begin{cases} 1 - u & m = 0 \\ 1 + u & m = 1 \\ P_m(u) - P_{m-2}(u) & m \geq 2 \end{cases} \quad (5)$$

has the property  $\tilde{P}_m(\pm 1) = 0, m \geq 2$ .  $M^u$  and  $N^v$  are the expansion orders along the direction of the current flows and along the transverse direction respectively.  $\tilde{C}_m$  and  $C_n$  are the scaling factors. To avoid the disadvantage that scaling all the functions to the maximum value of 1 doesn't perform well, the modified scaling factors are defined as

$$C_n = \sqrt{n + \frac{1}{2}} \quad (6)$$

$$\tilde{C}_m = \begin{cases} \frac{\sqrt{3}}{4} & m = 0, 1 \\ \frac{1}{2} \sqrt{\frac{(2m-3)(2m+1)}{2m-1}} & m \geq 2 \end{cases} \quad (7)$$

Thus, the  $u$ -directed current expansion is

$$J^u = \frac{1}{\mathcal{I}(u, v)} \left\{ \begin{aligned} & \sum_{n=0}^{N^v} [b_{0n}^u(1-u) + b_{1n}^u(1+u)] \tilde{C}_0 C_n P_n(v) \cdot e^{ik^i \cdot r} \\ & + \sum_{m=2}^{M^u} \sum_{n=0}^{N^v} b_{mn}^u \tilde{C}_m \tilde{P}_m(u) C_n P_n(v) \end{aligned} \right\} \quad (8)$$

Similar to the hierarchical basis function, the functions in the first part of (2) have a linear variation in the  $u$ -direction and are not zero at  $u = 1$  or  $u = -1$ . As a result of ensuring the normal current continuity across the  $v$ -directed edges, these functions can be called as edge functions. On the neighboring elements, the edge function matches with each other.

The functions in the second part of (2) are zero at the edges of the patches ( $u = \pm 1$ ). All of them are defined on a single patch. At the same time, they don't contribute to the normal continuity of the current. They display the  $M$ th order polynomial variations in the  $u$ -direction while  $M \geq 2$ . This part is usually referred as the patch function.

Due to the relationship with the direction of the incident wave, MPE basis functions are not suitable for incident direction scanning and the problem with multiple excitations.

## 2.2. Current Accuracy

MPE basis functions can be divided into two parts: the edge functions and the patch functions. Due to extracting the traveling wave phase

property, the edge functions are expressed as the multiplication of two factors: the amplitude factor and the phase factor. They represent the traveling wave property of the currents, and the patch functions show the standing wave terms. Such a rigorous current expansion has described the induced current distribution accurately.

There is an example of a metallic sphere at the frequency  $f = 600$  MHz. The radius is  $2\lambda_0$  ( $\lambda_0$  is the wavelength in free space).

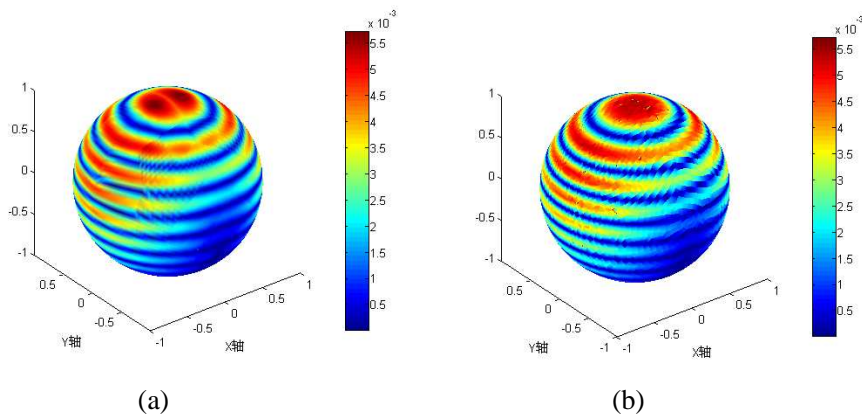


**Figure 1.** The real part of the induced current. (a) The result of using MPE basis functions. (b) The result of using Roof-top basis functions.

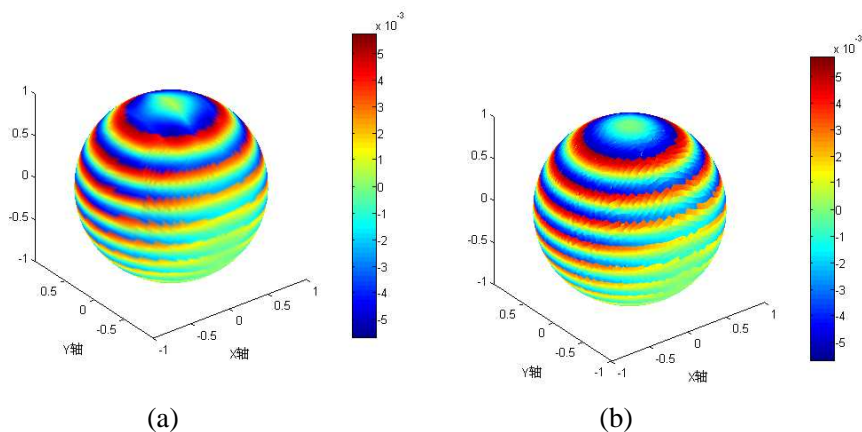


**Figure 2.** The imaginary part of the induced current. (a) The result of using MPE basis functions. (b) The result of using Roof-top basis functions.

It is placed at the origin of a rectangular  $xyz$ -coordinate system and illuminated by an  $x$ -polarized plane wave propagating in the  $z$ -direction. The induced currents on the surface obtained with MPE basis functions are compared with the results obtained with Roof-top basis functions. For MPE basis functions, the patch size is  $\lambda_0$ , and the corresponding expansion order is 2. The patch size is decreased to  $1/8\lambda_0$  while Roof-top basis functions are employed. Figure 1 and Figure 2 have shown the current distribution over the sphere. The results have a good agreement except the back scattering point. The differences may be caused by the coarse mesh. There are insufficient basis functions to model the current on a patch which is too large.

### 3. COMBINED WITH THE TDS FOR SOLVING THE THIN DIELECTRIC-COATED TARGETS

With the development of radar stealth and anti-stealth, the researches on the dielectric-coated metallic targets become more and more important. The dielectrics include both the electric media and the magnetic one. Sometimes, the thickness of the dielectric coating is quite small (e.g.,  $\tau \ll 0.1\lambda$ ,  $\lambda$  is the dielectric wavelength). For the situation, a lot of simplification can be done easily. The IBC has provided good numerical results while it has an ineluctable error and a great many physical restrictions to the practical applications. As an alternative, the TDS approximation combines with the explicit PEC boundary conditions can solve the scattering problems efficiently and accurately. It removes the need to solve the field in the dielectric coating.

#### 3.1. The Solution Combining with the TDS and MPE Basis Functions

For a dielectric-coated PEC system, the electric field can be described as follows:

$$[\mathbf{E}^{inc}(\mathbf{r}) + \mathbf{E}^{sca}(\mathbf{r})]_{\tan} = 0, \quad \mathbf{r} \in S_{pec} \quad (9)$$

The subscript “tan” stands for taking the tangential component of the vector. The scattering fields include the contributions from both metal components and dielectric components. The scattering fields from the PEC surface are given as

$$\mathbf{E}_{pec}^{sca}(\mathbf{r}) = ik_0\eta_0 \int_{S_{pec}} \bar{\bar{\mathbf{G}}}(\mathbf{r}, \mathbf{r}') \cdot \mathbf{J}_{pec}(\mathbf{r}') d\mathbf{S}' \quad (10)$$

And the fields from the dielectric are shown as

$$\mathbf{E}_{die}^{sca}(\mathbf{r}) = ik_0\eta_0 \int_V \bar{\bar{\mathbf{G}}}(\mathbf{r}, \mathbf{r}') \cdot \mathbf{J}_V(\mathbf{r}') d\mathbf{V}' - \int_V \nabla g(\mathbf{r}, \mathbf{r}') \times \mathbf{M}_V(\mathbf{r}') d\mathbf{V}' \quad (11)$$

$\mathbf{J}_V/\mathbf{M}_V$  is the polarization volume electric/magnetic current density in the volume  $V$ . And  $\bar{\bar{\mathbf{G}}}(\mathbf{r}, \mathbf{r}')$  is the dyadic Green function defined as

$$\bar{\bar{\mathbf{G}}}(\mathbf{r}, \mathbf{r}') = \left[ \bar{\bar{I}} - \frac{1}{k^2} \nabla \nabla' \right] g(\mathbf{r}, \mathbf{r}') \quad (12)$$

$g(\mathbf{r}, \mathbf{r}')$  is the scalar Green's function in free space which is defined by  $g(\mathbf{r}, \mathbf{r}') = \frac{e^{ik_0|\mathbf{r}-\mathbf{r}'|}}{4\pi|\mathbf{r}-\mathbf{r}'|}$ .

Following the equations below, and making some approximations, the final simplified integral Equation (19) can be obtained. Time dependence  $e^{-i\omega t}$  is assumed.

$$\mathbf{J}_v(\mathbf{r}') = i\omega\chi(\mathbf{r}')\mathbf{D}(\mathbf{r}') \quad (13)$$

$$\mathbf{M}_v(\mathbf{r}') = i\omega\xi(\mathbf{r}')\mathbf{B}(\mathbf{r}') \quad (14)$$

$$\mathbf{D}(\mathbf{r}') = \mathbf{D}_t(\mathbf{r}') + \hat{n}'\mathbf{D}_n(\mathbf{r}') \quad (15)$$

$$\mathbf{B}(\mathbf{r}') = \mathbf{B}_t(\mathbf{r}') + \hat{n}'B_n(\mathbf{r}') \quad (16)$$

where

$$\chi(\mathbf{r}') = \frac{1}{\varepsilon_r(\mathbf{r}')} - 1 \quad (17)$$

$$\xi(\mathbf{r}') = \frac{1}{\mu_r(\mathbf{r}')} - 1 \quad (18)$$

The fields are continuous across the PEC surface and almost no variation. Therefore, the approximations  $D_t(\mathbf{r}') \approx 0$ ,  $B_n(\mathbf{r}') \approx 0$  are introduced in the whole coating layer.

Then the scattering field from the dielectric is approximated by

$$\mathbf{E}_{die}^{sca}(\mathbf{r}) = iw\mu_0 \left[ \begin{aligned} & \int_S \hat{n}'\tau\chi g \nabla' \cdot \mathbf{J}_S dS' \\ & + \frac{\nabla}{k_0^2} \int_S \chi (g - g_\tau) \nabla' \cdot \mathbf{J}_S dS' \\ & + (1 - \mu_r) \int_S \tau \nabla g \times \hat{n}' \times \mathbf{J}_S dS' \end{aligned} \right] \quad (19)$$

where  $\tau$  represents the thickness of the dielectric,  $g_\tau(\mathbf{r}, \mathbf{r}') = g(\mathbf{r}, \mathbf{r}' + \tau\hat{n}')$ , and  $\mathbf{J}_S$  is the induced current density on the PEC surface.

By combining (9) with (10), (11), the incident electric field can be written as

$$\mathbf{E}^{inc}|_{\tan} = -iw\mu_0 \left[ \begin{aligned} & \frac{(1-\mu_r)\tau}{2} \cdot \mathbf{J}_S + \int_S g \cdot (\mathbf{J}_S + \hat{n}'\tau\chi\nabla' \cdot \mathbf{J}_S) dS' \\ & + \frac{\nabla}{k_0^2} \int_S (g + \chi g - \chi g_\tau) \nabla' \cdot \mathbf{J}_S dS' \\ & + (1 - \mu_r) \int_S \tau \nabla g \times \hat{n}' \times \mathbf{J}_S dS' \end{aligned} \right] \quad (20)$$

For the locally coated scatters,  $\tau$  and  $\chi$  are zero on the area where does not have the dielectric coating. Formula (20) is the electric field

integral equation (EFIE). Besides, the magnetic field integral equation (MFIE) is defined as

$$\hat{n} \times \mathbf{H}^{inc}(\mathbf{r}) = \frac{1}{2} \mathbf{J}_S - \hat{n} \times \left[ \int_S \nabla g \times \mathbf{J}_S dS' + \int_S k_0^2 (1 - \mu_r) \tau g \hat{n}' \times \mathbf{J}_S dS' + \int_S \nabla g \times \hat{n}' \tau \chi \nabla' \cdot \mathbf{J}_S dS' \right] \quad (21)$$

Finally, the combined field integral equation (CFIE) is defined by

$$\text{CFIE} = \alpha \text{EFIE} + \eta (1 - \alpha) \text{MFIE} \quad (22)$$

$\alpha$  is the combine coefficient and  $\eta$  is the wave impedance in free space.

Thus,  $\mathbf{J}_S$  can be expanded by using the MPE basis function

$$\mathbf{J}_S = \sum_{i=1}^N a_i \mathbf{j}_i(\mathbf{r}) \quad (23)$$

where  $\mathbf{j}_i(\mathbf{r})$  is the basis function, and the divergence of  $\mathbf{j}_i(\mathbf{r})$  can be expressed as

$$\begin{aligned} \nabla \cdot \mathbf{j}_i(\mathbf{r}) = & e^{i\mathbf{k}^i \cdot \mathbf{r}} \cdot \nabla \cdot \left\{ \frac{1}{\mathcal{J}(u,v)} \sum_{n=0}^{N^v} [b_{0n}^u (1-u) + b_{1n}^u (1+u)] \tilde{C}_0 C_n P_n(v) \right\} \\ & + i\mathbf{k}^i e^{i\mathbf{k}^i \cdot \mathbf{r}} \left\{ \frac{1}{\mathcal{J}(u,v)} \sum_{n=0}^{N^v} [b_{0n}^u (1-u) + b_{1n}^u (1+u)] \tilde{C}_0 C_n P_n(v) \right\} \\ & + \nabla \cdot \left[ \frac{1}{\mathcal{J}(u,v)} \sum_{m=2}^{M^u} \sum_{n=0}^{N^v} b_{mn}^u \tilde{C}_m \tilde{P}_m(u) C_n P_n(v) \right] \quad (24) \end{aligned}$$

**Table 1.** Expansion order for the dielectric-coated sphere.

Patch size ( $\lambda_0$ )	Order of Higher order hierarchical Legendre basis	Order of MPE basis
0.5	3	2
0.8	4	3
1.3	5	3
1.5	6	4
1.7	7	4
2	8	5
2.4	9	6
3	10	8

With the Formulation (20), (21) and (22), the Galerkin's testing method is applied to transform integral equations into a system about linear equations.

For a coated sphere, the average patch size and the corresponding expansion order are listed in Table 1. The expansion order for MPE and higher order hierarchical Legendre basis functions are displayed together. From the table, the distinction between the MPE basis function and the higher order hierarchical Legendre basis function are clear. The expansion order of the MPE basis function is lower than that of the higher order hierarchical basis function for the same patches. Particularly, the advantage is more obvious for the larger patches.

When applied to an object that has a complex structure, the expansion order must be increased properly. The order shown in Table 1 would not be enough to model the edge current in the complex configuration.

### 3.2. Numerical Results

The examples shown below are analyzed by the computer which has 8 processors. In addition, all the MPE results shown are obtained with 2 order basis functions.

Firstly, scattering by a PEC sphere of radius  $R = 3$  m coated with a dielectric material of thickness 5 mm is considered. The frequency is set to 1 GHz ( $\lambda_0 = 0.3$  m) and  $\epsilon_r = (4.5, -0.15)$ ,  $\mu_r = (0.16, -0.09)$ . The sphere is illuminated by an incident plane wave ( $\theta = 0^\circ$  and  $\varphi = 0^\circ$  in spherical coordinates). The mesh for this example includes 5600 elements, with an average edge length of  $0.5\lambda_0$ . The CFIE is solved with equally weighted EFIE and MFIE parts ( $\alpha = 0.5$ ). The bi-static radar cross section (RCS) computed in the  $\varphi = 0^\circ$  plane is calculated.

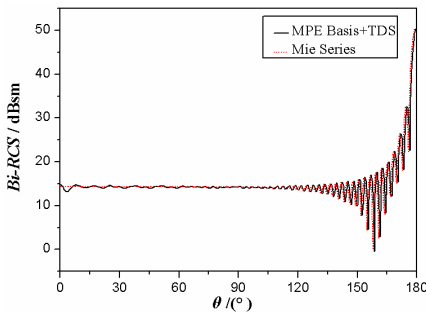


**Figure 3.** Bistatic RCS for the coated sphere.

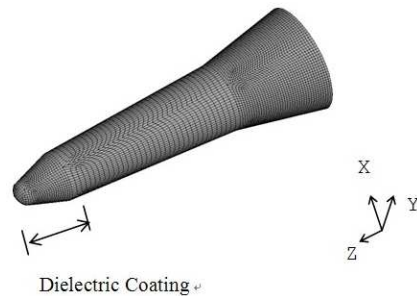


**Figure 4.** Curvilinear mesh of the coated missile-like object.

Figure 3 shows the excellent agreement with the corresponding exact result. Only 44760 unknowns are needed to solve the problem. In contrast, if RWG basis functions are employed, 626400 unknowns would be required.

Secondly, the scattering by a missile-like object locally coated with absorbing materials [14] is presented. The model is shown in Figure 4. The frequency is 20 GHz. The major axis of the target is about  $52.5\lambda_0$  ( $\lambda_0 = 15$  mm). Only the front end of the object is coated with dielectric ( $\epsilon_r = (29.78, -2.31)$ ,  $\mu_r = (1.87, -1.96)$ ). The coating thickness is 0.1 mm. The surface of the object is modeled with 10178 curvilinear quadrilateral patches. The bi-static RCS is computed for an incident wave in the  $\varphi = 0^\circ$  plane as a function of  $\theta$ . The EFIE is employed.

The results of MPE basis function combing with the TDS are indicated by the solid curve, whereas the results of RWG basis function combing with the IBC are shown by the curve (' $\Delta$ '). There are good agreements between the two results. Another result is revealed for the RWG basis function combing with the TDS (the dot line). Note that the MPE results compare well with the RWG results. The errors in Figure 5 can be eliminated with a much finer discretization in the edge

**Table 2.** Results for the missile using different bases.

Basis/ Method	Unknown	Iteration Step/Method	Time of Impedance Matrix Calculation (h)	Time of Iteration (h)	CPU Time (h)
RWG/TDS +MLFMA	1,819,035	752/GMRES	1.65	7.17	9.7
MPE/TDS +MoM	81,416	208/CG	5.86	0.33	6.2

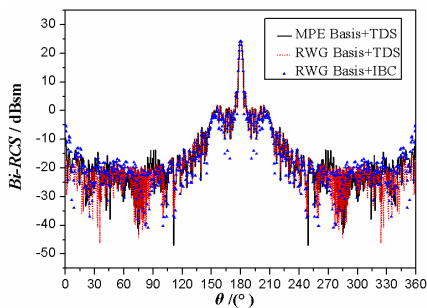


**Figure 5.** Bistatic RCS for the coated missile-like object.

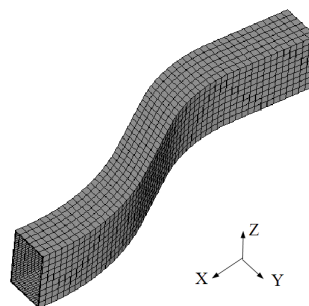


**Figure 6.** The model of the locally coated cavity.

of the tail. As defined in the large patches which need a great deal integral points, most of the time is consumed in filling the impedance matrix. For the RWG basis function, a same number of unknowns would be required using the TDS solution and the IBC solution. As seen in Table 2, the MPE results that require 81416 unknowns compare well with that of the RWG results which require 1819035 unknowns. The savings in the number of unknowns are very significant.

At last, a locally coated s-shaped cavity of 2 GHz is analyzed. The configuration used in this section is shown in Figure 6. The length, width and height are  $32\lambda_0$ ,  $3.7\lambda_0$ ,  $5\lambda_0$  ( $\lambda_0 = 0.15$  m) respectively. The thickness of the metal area is about  $0.35\lambda_0$ . The inner surface of the model is coated with the absorbing materials, which have the dielectric parameters  $\epsilon_r = (18.06, -1.06)$ ,  $\mu_r = (4.07, -1.97)$ . And the dielectric thickness is 1.0 mm. The cavity is illuminated by an  $H$ -Polarized plane wave from the direction specified by  $(90^\circ, 0^\circ)$ . 4427 curvilinear patches are used to represent the whole surface totally. The bi-static RCS in the  $\theta = 90^\circ$  plane is studied. And the EFIE is used.

**Table 3.** Results for the cavity using different bases.

Basis/ Method	Unknown	Iteration Step/Method	Time of Impedance Matrix Calculation (h)	Time of Iteration (h)	CPU Time (h)
RWG/ MLFMA	568,191	276/GMRES	0.45	2.66	3.55
MPE/ MoM	35,406	501/CG	1.05	0.70	2.10

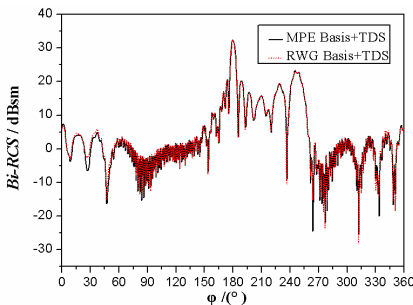


**Figure 7.** Bistatic RCS for the locally coated cavity.

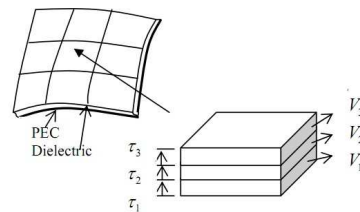


**Figure 8.** The 3 layered model of modified TDS approximation.

Table 3 has shown the number of unknowns, iteration step and CPU time. The results shown by the solid curve are obtained with MPE basis functions. And the dot curve is the results calculated by RWG basis functions. From Figure 7, the results compare well with each other. The reduction of the unknowns by using MPE basis functions is remarkable. The number of unknowns is reduced by 93.7% compared with that of the RWG results.

#### 4. MODIFIED TDS FOR SOLVING THE COATED TARGETS

Considering the characteristic that the field varies slowly in each dielectric layer, the surface integral is used to instead of the volume integral in Formula (19). During the procedure, Green's functions are the kernel of the integral. As the function of the position coordinate, the values of Green's functions change quickly, particularly when the distance between the field point and the source point is very short. The error is introduced while the surface integral is used approximately. Therefore, the accuracy of the TDS approximation is highly dependent on the application of Green functions.

Generally, the dielectric thickness adapted to the traditional TDS approximation is much less than  $0.1\lambda$ . When the material is a little thicker, but is still thin enough compared with the dielectric wavelength, the approximation errors introduced in the application of the Green's function should not be neglected. The Green's function should be chosen to be more closely within the material region.

Aimed to improve the calculation precision when the dielectric coating is thicker, the dielectric layers can be considered as the sum of 3 or more layers. For the material of the layers are the same one, the tangential components of the electromagnetic fields still are zero at the interface. For example, the dielectric domain  $V$  can be divided into 3 parts averagely:  $V_1, V_2, V_3$ . The geometric model is shown in Figure 8.

##### 4.1. The Modified TDS

Then the Equation (11) can be rewritten as

$$\begin{aligned} \mathbf{E}_{die}^{sca}(\mathbf{r}) = & ik_0\eta_0 \sum_{j=1}^3 \int_{V_j} \bar{\bar{\mathbf{G}}}(\mathbf{r}, \mathbf{r}') \cdot \mathbf{J}_V(\mathbf{r}') d\mathbf{V}' \\ & - \sum_{j=1}^3 \int_{V_j} \nabla g(\mathbf{r}, \mathbf{r}') \times \mathbf{M}_V(\mathbf{r}') d\mathbf{V}' \end{aligned} \quad (25)$$

Thus, the scattering field from the dielectric is approximated by

$$\mathbf{E}_{die}^{sca}(\mathbf{r}) = iw\mu_0 \left[ \begin{aligned} & \sum_{i=1}^3 \int_S \hat{\mathbf{n}}' \tau_i \chi_i g_{\tau_{i-1}} \nabla' \cdot \mathbf{J}_S dS' \\ & + \frac{\nabla}{k_0^2} \sum_{i=1}^3 \int_S \chi_i (g_{\tau_{i-1}} - g_{\tau_i}) \nabla' \cdot \mathbf{J}_S dS' \\ & + (1 - \mu_r) \sum_{i=1}^3 \int_S \tau_i \nabla g_{\tau_{i-1}} \times \hat{\mathbf{n}}' \times \mathbf{J}_S dS' \end{aligned} \right] \quad (26)$$

where  $\tau_i$  and  $\chi_i$  represent the thickness and  $\chi$  of the  $i$ th layer respectively, and  $\mathbf{J}_S$  is the induced current density. In this paper,  $\tau_1$ ,  $\tau_2$ , and  $\tau_3$  are all equal to one third of the thickness of the whole dielectric coatings ( $\tau_i = (\tau_1 + \tau_2 + \tau_3)/3$ ).  $g_{\tau_i}(\mathbf{r}, \mathbf{r}') = g(\mathbf{r}, \mathbf{r}' + \tau_i \hat{\mathbf{n}}')$ , ( $i = 1, 2, 3$ ). And  $g_{\tau_0}(\mathbf{r}, \mathbf{r}') = g(\mathbf{r}, \mathbf{r}')$ .

The incident electric field can be rewritten as

$$\mathbf{E}^{inc}|_{tan} = -iw\mu_0 \left[ \begin{aligned} & \sum_{i=1}^3 \frac{(1-\mu_r)\tau_i}{2} \cdot \mathbf{J}_S \\ & + \int_S g \cdot \mathbf{J}_S dS' + \frac{\nabla}{k_0^2} \int_S g \cdot \nabla' \cdot \mathbf{J}_S dS' \\ & + \sum_{i=1}^3 \int_S \hat{\mathbf{n}}' \tau_i \chi_i g_{\tau_{i-1}} \nabla' \cdot \mathbf{J}_S dS' \\ & + \frac{\nabla}{k_0^2} \sum_{i=1}^3 \int_S \chi_i (g_{\tau_{i-1}} - g_{\tau_i}) \nabla' \cdot \mathbf{J}_S dS' \\ & + (1 - \mu_r) \sum_{i=1}^3 \int_S \tau_i \nabla g_{\tau_{i-1}} \times \hat{\mathbf{n}}' \times \mathbf{J}_S dS' \end{aligned} \right] \quad (27)$$

The incident magnetic field is defined as

$$\begin{aligned} & \hat{\mathbf{n}} \times \mathbf{H}^{inc}(\mathbf{r}) \\ & = \frac{1}{2} \mathbf{J}_S - \hat{\mathbf{n}} \times \left[ \begin{aligned} & \int_S \nabla g \times \mathbf{J}_S dS' + \sum_{i=1}^3 \int_S k_0^2 (1 - \mu_r) \tau_i g_{\tau_{i-1}} \hat{\mathbf{n}}' \times \mathbf{J}_S dS' \\ & + \sum_{i=1}^3 \int_S \nabla g_{\tau_{i-1}} \times \hat{\mathbf{n}}' \tau_i \chi_i \nabla' \cdot \mathbf{J}_S dS' \end{aligned} \right] \end{aligned} \quad (28)$$

Formulas (27) and (28) are the EFIE and MFIE respectively. With the Galerkin's testing employed for the Equations (27) and (28), the MoM matrix is obtained.

## 4.2. Numerical Results

When the dielectric is thicker, such as  $0.2\lambda$  ( $\lambda$  is the dielectric wavelength), the problem would not be analyzed exactly by using the traditional TDS approximation. Nevertheless, the modified TDS

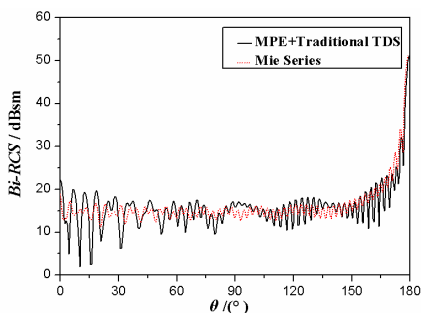


**Figure 9.** Bistatic RCS for the coated sphere obtained with the traditional TDS model.

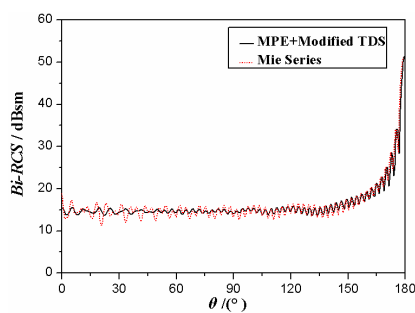


**Figure 10.** Bistatic RCS for the coated sphere obtained with the modified TDS model.

approximation has the ability to do it. The results given in Figure 10 have shown the good precision.

The sphere considered in the example is modeled by 5600 patches at 1 GHz. The dielectric thickness is up to 40 mm ( $0.18\lambda$ ). The parameters of the coating material are  $\epsilon_r = (2.0, -0.005)$  and  $\mu_r = (1.0, 0.0)$ . Both the MPE results are obtained with 2 order basis functions. The bi-static RCS in the  $H$ -plane for a dielectric-coated sphere is shown in Figure 9 and Figure 10. CG iteration and the CFIE are used.

In the figures above, results are present for different cases. Case 1: the RCS result (the solid curve) solved with the solution in Section 3 is displayed in Figure 9; Case 2: the RCS result (the solid one) obtained with the modified solution is shown in Figure 10. As seen, the results of the second case agree with the Mie series results very well. However, the errors between the results of the two solutions are obvious in Figure 9. Without increasing the number of unknowns and memory requirement, the more accurate results can be obtained with the modified solution proposed in this section. The validity of the modified solution is demonstrated.

## 5. CONCLUSION

A new set of basis function called as the MPE basis function is considered, and also the expressions of MPE basis functions for combining with the TDS approximation are given. The new basis functions have the ability to describe the standing wave and travelling wave properties at the same time. This allows the basis function

can be defined on large patches. For electrically large scattering problems, the approach proposed in this paper reduces the number of unknowns compared with the traditional method. The validity, accuracy and efficiency of the new approach have been demonstrated with several examples. In addition, some modifications based on the TDS approximation are proposed to solve the scatters which have thicker dielectric coatings (e.g.,  $0.2\lambda$ ). There is also an example to confirm the validity of the modified solution. As a consequence, an electrically large dielectric-coated problem can be solved efficiently. It is shown by the numerical results that the calculation capability of MoM is improved with fewer unknowns. Combining with the fast algorithm, the approach can be used to analyze the electrically large targets rapidly and accurately.

## ACKNOWLEDGMENT

This work was supported by the National Natural Science Foundation of China under Project No. NSFC 60931004.

## REFERENCES

1. Shi, Y., X. Luan, J. Qin, C. Lv, and C.-H. Liang, "Multilevel green's function interpolation method solution of volume/surface integral equation for mixed conducting/bi-isotropic objects," *Progress In Electromagnetics Research*, Vol. 107, 239–252, 2010.
2. Araujo, M. G., J. M. Taboada, J. Rivero, and F. Obelleiro, "Comparison of surface integral equations for left-handed materials," *Progress In Electromagnetics Research*, Vol. 118, 425–440, 2011.
3. Cui, Z.-W, Y.-P. Han, and M.-L. Li, "Solution of CFIE-JMCFIE using parallel MOM for scattering by dielectrically coated conducting bodies," *Journal of Electromagnetic Waves and Applications*, Vol. 25, No. 2–3, 211–222, 2011.
4. Bui, V. P., X.-C. Wei, and E. P. Li, "An efficient simulation technology for characterizing the ultra-wide band signal propagation in a wireless body area network," *Journal of Electromagnetic Waves and Applications*, Vol. 24, No. 17–18, 2575–2588, 2010.
5. Kolpakov, A. A. and A. G. Kolpakov, *Capacity and Transport in Contrast Composite Structures: Asymptotic Analysis and Applications*, Taylor & Francis Group Boca Raton, 2010.
6. He, S., Z. Nie, and J. Hu, "Numerical solution of scattering from thin dielectric-coated conductors based on TDS approximation

- and EM boundary conditions,” *Progress In Electromagnetics Research*, Vol. 93, 339–354, 2009.
7. Chiang, I. T. and W. C. Chew, “Thin dielectric sheet simulation by surface integral equation using modified RWG and pulse bases,” *IEEE Trans. Antennas Propag.*, Vol. 54, 1927–1934, Jul. 2006.
  8. Chiang, I. T. and W. C. Chew, “A coupled PEC-TDS surface integral equation approach for electromagnetic scattering and radiation from composite metallic and thin dielectric objects,” *IEEE Trans. Antennas Propag.*, Vol. 54, 3511–3516, Nov. 2006.
  9. Kolundzija, B. M. and D. S. Sumic, “Hierarchical conjugate gradient method applied to MoM analysis of electrically large structures,” *Proceedings of the 2004 international IEEE APS Symposium*, Vol. 4, 4455–4458, Jun. 2004.
  10. Nie, Z., S. Yan, and S. He, “On the basis functions with traveling wave phase factor for efficient analysis of scattering from electrically large targets,” *Progress In Electromagnetics Research*, Vol. 85, 83–114, 2008.
  11. Taboada, J. M., M. G. Araujo, J. M. Bertolo, L. Landesa, F. Obelleiro, and J. L. Rodriguez, “MLFMA-FFT parallel algorithm for the solution of large-scale problems in electromagnetics,” *Progress In Electromagnetics Research*, Vol. 105, 15–30, 2010.
  12. Jørgensen, E., J. L. Volakis, and P. Meincke, “Higher order hierarchical Legendre basis functions for electromagnetic modeling,” *IEEE Trans. Antennas Propag.*, Vol. 52, No. 11, 2985–2995, Nov. 2004.
  13. Eibert, T. F., Ismatullah, E. Kaliyaperumal, and C. H. Schmidt, “Inverse equivalent surface current method with hierarchical higher order basis functions, full probe correction and multi-level fast multipole acceleration,” *Progress In Electromagnetics Research*, Vol. 106, 377–394, 2010.
  14. Ding, D.-Z. and R.-S. Chen, “Electromagnetic scattering by conducting BOR coated with chiral media above a lossy half-space,” *Progress In Electromagnetics Research*, Vol. 104, 385–401, 2010.